This is a preprint, the final version is subject to change, of the American Mineralogist (MSA)
Cite as Authors (Year) Title. American Mineralogist, in press.
(DOI will not work until issue is live.) DOI: http://dx.doi.org/10.2138/am-2017-5919

Revision 3 to American Mineralogist

Mengxianminite, ideally $Ca_2Sn_2Mg_3Al_8[(BO_3)(BeO_4)O_6]_2$, a new borate mineral from Xianghualing skarn, Hunan Province, China

CAN RAO[1,2,*], FRÉDÉRIC HATERT[2], FABRICE DAL BO[2], RUCHENG WANG[3], XIANGPING GU[4] AND MAXIME BAIJOT[2]

[1] School of Earth Sciences, Zhejiang University, Hangzhou, 310027, China

[2] Laboratoire de Minéralogie, B18, Université de Liège, B–4000 Liège, Belgium

[3] State Key Laboratory for Mineral Deposits Research, School of Earth Sciences and Engineering, Nanjing University, Nanjing, 210046, China

[4] School of Earth Sciences and Info-physics, Central South University, Changsha, 410083, China

*E-mail: canrao@zju.edu.cn

ABSTRACT

Mengxianminite, ideally $Ca_2Sn_2Mg_3Al_8[(BO_3)(BeO_4)O_6]_2$, is a new borate mineral from Xianghualing skarn, Hunan Province, southern China. It occurs in the hsianghualite vein of Xianghualing skarn, associated with fluorite, phlogopite, hsianghualite, magnetite, dravite, magnesiotaaffeite-2*N'*2*S* and calcite. Mengxianminite forms subhedral to euhedral green crystals from 20 to 200 μm long, translucent to transparent, with a vitreous luster. The crystals show perfect cleavage on {100} and good cleavage on {010}, and do not fluoresce in long- or short-wave ultraviolet light. The estimated Mohs hardness is 8, and the tenacity is brittle with irregular fracture. The calculated density is 4.170 g/cm^3. Optically, mengxianminite is biaxial (–), with α = 1.80(2), β = 1.83(2), γ = 1.84(2) (589 nm). The mean chemical composition of mengxianminite (Be and B were measured by secondary ion mass spectrometry, average of 6 electron microprobe analyse points and in wt%) is Al_2O_3 40.00, SnO_2 25.96, MgO 6.57, CaO 8.56, FeO 4.83, B_2O_3 6.53, BeO 4.37, ZnO 1.81, MnO 1.23, Na_2O 1.13, TiO_2 0.10, SiO_2 0.04, sum 101.12 with a corresponding empirical formula calculated on the basis of 26 O atoms of $(Ca_{1.64},Na_{0.39})_{\Sigma 2.03}(Sn_{1.85},Zn_{0.24})_{\Sigma 2.09}(Mg_{1.75},Fe_{0.72},Al_{0.42},Mn_{0.19},Ti_{0.01})_{\Sigma 3.09}Al_8[(B_{1.01}O_3)(Be_{0.94}O_4)O_6]_2$. The strongest 8 lines of the powder XRD pattern [d in Å (I)(hkl)] are: 3.000(35)(16 2 0); 2.931(100)(17 1 1); 2.475(29)(022); 2.430(30)(13 3 1); 2.375(100)(14 0 2/640); 2.028(52)(21 3 1); 1.807(35)(913); 1.530(98)(14 6 0/15 3 3). Mengxianminite is orthorhombic, space group *Fdd*2; unit-cell parameters refined from single-crystal X-ray diffraction data are: *a* = 60.699 (4), *b* = 9.914 (1), *c* = 5.745 (1) Å, *V* = 3457.4 (4) Å^3, Z = 8. The structure of mengxianminite is characterized by the alternating O-T1-O-T2-O'-T2 layers stacked along

the *a* axis, which are equal to two alternating modules: the module A (O-T1-O) corresponding to the spinel module with an additional O layer (AlO_6 octahedra layer), and the module B (T2-O'-T2) showing the simplified formula $CaSnAl(BeO_4)(BO_3)$, where SnO_6 octahedra are isolated in the T2 layers, connected via BeO_4 and CaO_{11} groups, and AlO_6 edge-sharing octahedra in the O' layer form chains running along the {011} or $\{0\bar{1}1\}$ direction, connected in the *c* direction by the BO_3 triangular groups. Mengxianminite is the first borate mineral with both Sn and Be, likely crystallized under F-rich conditions at late stages of the Xianghualing skarn.

Key words: mengxianminite, new mineral, Xianghualing skarn, Hunan province, China.

INTRODUCTION

A new mineral species, mengxianminite, ideally $Ca_2Sn_2Mg_3Al_8[(BO_3)(BeO_4)O_6]_2$, has been found in the Xianghualing sharn, Linwu County, Hunan Province (southern China). We should point out that mengxianminite was firstly reported as a Sn-bearing oxide from the hsianghualite vein of the Xianghualing skarn, Hunan Province, southern China by Huang et al. (1986, 1988). However, it was not properly characterized by these authors. Moreover, it was not listed either as a valid or an invalid unnamed mineral (Smith and Nickel 2007). Since the "mengxianminite" reported by Huang et al. (1986, 1988) is from the same locality and has a similar chemical composition and crystal-structure, we have retained the name "mengxianminite" for the Be-B-Sn mineral described here.

Optical microscopy, electron probe microanalysis, secondary-ion mass spectrometry (SIMS), X-ray diffraction, Raman and infrared spectroscopy were used to determine its petrographic features, chemical composition and crystal structure. The new mineral is named after "Meng Xianmin" (1900-1969), a famous geologist in China, who devoted himself to work on mineral identification and theory of mineralization in deposits of non-ferrous metals, and made significant contributions to the research of ore deposits in China. The species and the name have been approved by the International Mineralogical Association, Commission on New Minerals, Nomenclature and Classification (CNMNC) (IMA 2015-70) (Rao et al. 2016). The type sample of mengxianminite, used to collect the electron-microprobe data, is stored in the Geological Museum of China, No. 16, Yangrou Hutong, Xisi, Beijing 100031, People's Republic of China. Catalogue number of material is M13293. The co-type sample used for the single-crystal structure and optical measurements is stored at the Laboratory of Mineralogy, University of Liège, Belgium (catalog number 20395). This paper describes the physical and chemical properties of mengxianminite and its crystal structure determined from the single-crystal X-ray diffraction data, and discusses the origin and implications.

OCCURRENCE

Mengxianminite was found in the Xianghualing skarn, Hunan Province, southern China, which is located at longitude E 112°34', latitude northeast of 25°26', about 20 km northeastern of Linwu County. In this area, the principal unit is the Laiziling granite, which intrudes sandstone and sandy shale of Tiaomajian Formation, and limestone and dolomitic limestone of Qiziqiao Formation. A vertical zonation is well developed from the deeper level

upwards to the top of the Laiziling mountain peak: protolithionite granite zone, leucogranite zone, albite granite zone, greisen zone, massive quartz zone and pegmatoid stockscheider zone. The U-Pb dating of zircon of the protolithionite granite gave 155 Ma (Zhu et al. 2011). The Xianghualing skarn was typically distributed around the Laiziling granite, and/or along the related tectonic faults, formed a tin-polymetallic (Sn-W-Be-Li) deposit, which is the type locality of hsianghualite $Ca_3Li_2Be_3(SiO_4)_3F_2$ (Huang et al. 1958), liberite $Li_2Be(SiO_4)$ (Chao 1964) and ferrotaaffeite-2*N*'2*S* $BeFe_3Al_8O_{16}$ (Yang et al. 2012). The Laiziling granite with high levels of Li, Be, Sn, W, Rb, Nb, and Ta, was generally regarded as the main source of the Xianghualing orebodies. The average concentrations of Be and Sn in the Laiziling granite are 16 ppm and 65 ppm, respectively (Zhong 2014).

Mengxianminite occurs in the hsianghualite vein of the Xianghualing skarn, which is located in the exocontact zone of the Laiziling granite and in the Middle-Upper Devonian carbonate rocks of the Qiziqiao Formation. It forms subhedral to euhedral crystals ranging from 20 to 200 μm in size (Fig. 1). In some cases, mengxianminite was replaced by late fluorite along cleavage planes, resulting in the local precipitation of small cassiterite crystals (Fig. 1a). Other associated minerals include phlogopite, hsianghualite, magnetite, dravite, magnesiotaaffeite-2*N*'2*S* and calcite.

PHYSICAL AND OPTICAL PROPERTIES

Mengxianminite is green and shows well-developed or perfect cleavage on {100} and good cleavage on {010} (Fig. 1b). It does not show fluorescence in long- or short-wave ultraviolet light. The crystals are translucent to transparent with vitreous luster. The Mohs

hardness is about 8 by comparison with the hardness of magnesiotaaffeite-2*N*2*S*, the tenacity is brittle with irregular fracture. Based on the empirical formula and single-crystal unit-cell parameters, the calculated density is 4.170 g/cm^3. Optically, mengxianminite is biaxial negative, with α = 1.80(2), β = 1.83(2), γ = 1.84(2) (589 nm). The calculated 2*V* is 60°, and optical orientation: α, β and γ are parallel to crystallographic *a*, *b* and *c*, respectively. The pleochroism is *X* = light green, *Y* = light green, and *Z* = colorless. According to the calculated density and the measured indexes of refraction, the compatibility index $[1 - (K_P/K_C)]$ is −0.036, and corresponds to the "excellent" category (Mandarino 1981).

RAMAN AND INFRARED SPECTROSCOPIES

Raman spectra of mengxianminite were collected using a LabRAM HR evolution Laser Raman microprobe in the School of Earth Sciences at Zhejiang University. A 532 nm laser with a power of 50 mW at the sample surface was used for exciting the radiation. Silicon (520 cm^{-1} Raman shift) was used as a standard. Raman spectra were acquired from 100 to 4000 cm^{-1} and the accumulation time of each spectrum is 60 s. The Raman spectra were obtained on single crystals of mengxianminite on polished thin section chips. It is characterized by the strong sharp peak at 754 cm^{-1}, medium sharp peaks at 1009, 806, 722, 606, and 506 cm^{-1}, and weak sharp peaks at 553 and 156 cm^{-1} (Fig. 2). The Raman shifts at 722 and 533 cm^{-1} show the stretching and bending modes of (BO_3) groups in the structure, and the Raman shift at 754 cm^{-1} is related to the stretching mode of (AlO_6) groups. The Be-O vibration modes are probably at 1009 and 156 cm^{-1}, and the Raman shift at 606 cm^{-1} probably corresponds to

142 Sn-O vibration. The Ca-O and Mg-O vibration modes are probably at 806 and 506 cm^{-1},
143 respectively.

144 An infrared spectrum (400 to 5600 cm^{-1}) was obtained on a Nicolet iso50 FTIR
145 spectrometer coupled with a Continuum microscope installed in the School of Earth Sciences
146 at the Zhejiang University, using a KBr beam-splitter and a liquid-nitrogen cooled MCT-A
147 detector. All measurements were carried out using reflection technique. The representative
148 infrared spectrum of mengxianminite is given in Figure 3. The bands at 1426, 1328, 1155,
149 1050 and 918 cm^{-1} correspond to the stretching vibrations of (BO_3) groups, the band at 711
150 cm^{-1} to the vibrations of (BeO_4) tetrahedra, and the band at 672 cm^{-1} to the bending of (AlO_6)
151 octahedra. The infrared spectrum also gives no evidence for the presence of either H_2O or OH
152 in the structure of mengxianminite.
153

154 ## CHEMICAL COMPOSITION

155 Quantitative elemental microanalyses of mengxianminite were conducted with a JEOL
156 JXA-8100M electron microprobe (WDS mode, 15 kV, 20 nA, beam diameter 1μm) at the
157 Second Institute of Oceanography, State Oceanic Administration (Hangzhou, China).
158 Standards for the analysis were topaz (Al *Kα* and Si *Kα*), cassiterite (Sn *Lα*), forsterite (Mg
159 *Lα*), fayalite (Fe *Kα*), synthetic $MnTiO_3$ (Mn *K*α and Ti *K*α), synthetic ZnO (Zn *Kα*), albite
160 (Na *Kα*), K-feldspar (K *Kα*) and synthetic $CaSiO_3$ (Ca *Kα*). The low analytical total is due to
161 the presence of large amounts of BeO and B_2O_3 contents.

162 The BeO and B_2O_3 contents were measured using secondary ion mass spectrometry with
163 a CAMECA NanoSIMS 50L at the Institute of Geology and Geophysics, China Academy of

Sciences. A relatively high beam current (500 pA) was used initially to pre-sputter 12 μm ×12 μm of the matrix area. The measurements were undertaken in raster imaging mode by scanning a focused Cs^+ primary ion beam (30 pA, 0.5 μm diameter) over 10 μm × 10 μm matrix area within the pre-sputtered regions. Negative secondary ions $^{9}Be^-$, $^{10}B^-$,$^{11}B^-$, $^{16}OH^-$, $^{18}O^-$ were collected simultaneously, along with secondary electrons (SE). In order to be used as a standard for Be and B, the structure and composition of hambergite from the Xianghualing skarn was confirmed as the F-free end-member $Be_2(BO_3)(OH)$ by single crystal XRD in the Laboratory Mineralogy, Liège University (Belgium). The calibration factors for Be and B in the standard were obtained through the calculation of the experimental Be and B ions yield, having chosen O as the inference element for the matrix. Thus we derived the ratios (Be/O) and (B/O), defined as $(Be^-/O^-)/((Be(at.)/O(at.))$ and $(B^-/O^-)/((B(at.)/O(at.))$, respectively, where Be^-, B^- and O^- are the current intensities detected at the electron multiplier and (at.), are the elemental atomic concentration. The ratios (Be/O) and (B/O) were then used to calculate the Be and B concentration in mengxianminite. Additionally, lithium was confirmed to be absent from the mineral.

The chemical composition of mengxianminite is given in Table 1. The empirical formula, calculated on the basis of 26 O atoms per formula unit, is: $(Ca_{1.64},Na_{0.39})_{\Sigma 2.03}(Sn_{1.85},Zn_{0.24})_{\Sigma 2.09}(Mg_{1.75},Fe_{0.72},Al_{0.42},Mn_{0.19},Ti_{0.01})_{\Sigma 3.09}Al_8[(B_{1.01}O_3)(Be_{0.94}O_4)O_6]_2$, yielding the simplified formula of $Ca_2Sn_2Mg_3Al_8[(BO_3)(BeO_4)O_6]_2$. The ideal formula requires Al_2O_3 38.41 wt%, SnO_2 28.38 wt%, MgO 11.39 wt %, CaO 10.56 wt%, B_2O_3 6.56 wt% and BeO 4.71 wt%, total 100.00 wt%.

X-RAY POWDER DIFFRACTION

The powder XRD pattern of mengxianminite was collected from micro-diffraction data of two crystals, on a RIGAKU D/max Rapid IIR micro-diffractometer (CuKα, λ = 1.54056 Å) at the School of Earth Sciences and Info-physics, Central South University, China. The micro-diffractometer was operated with a Gandolfi-like motion, under 48 kV and 25 mA, using a 0.05 mm diameter collimator; total exposure time was 2 h. The structural model of single crystals (see below) was used to index the powder XRD pattern of mengxianminite (Table 2). Calculated intensities were obtained from the structural data with POWDER CELL (Krauz and Nolze 1996). The stronger eight lines of the powder XRD pattern [d in Å (I)(hkl)] are: 3.000(35)(16 2 0); 2.931(100)(17 1 1); 2.475(29)(022); 2.430(30)(13 3 1); 2.375(100)(14 0 2/640); 2.028(52)(21 3 1); 1.807(35)(913); 1.530(98)(14 6 0/15 3 3). Because of small size of the crystals and large beam diameter (100 μm), some peaks of mengxianminite overlap with phlogopite and fluorite. Unit-cell parameters calculated from powder XRD data of mengxianminite are: a = 60.83(14), b = 9.835(4), c = 5.742(1) Å, V = 3435(10) Å^3, Z = 8, and space group is *Fdd*2.

CRYSTAL STRUCTURE DETERMINATION

Single-crystal X-ray diffraction data, aimed to perform a structure refinement of mengxianminite (CIF[1] available on deposit), were collected on an Agilent Technologies Xcalibur four-circle diffractometer, equipped with an EOS CCD area-detector (University of Liège, Belgium), on a crystal fragment measuring 0.139 x 0.108 x 0.088 mm. Some 420

[1] Deposit item AM-?, CIF

frames with a spatial resolution of 1° were collected by the φ/ω scan technique, with a counting time of 90 s per frame, in the range 5.34° < 2θ < 53.31°. A total of 7315 reflections were extracted from these frames, corresponding to 2063 unique reflections. Unit cell parameters refined from these reflections are a = 60.699 (4), b = 9.914 (1), c = 5.745 (1) Å, α = β = γ = 90º, V = 3457.4 (4) Å^3, Z = 8, space group *Fdd*2. Crystal data, data-collection information, and refinement details for mengxianminite are provided in Table 3. Data were corrected for Lorentz, polarisation and absorption effects, the last with an empirical method using the SCALE3 ABSPACK scaling algorithm included in the CrysAlisRED package (Oxford Diffraction 2007). Scattering curves for neutral atoms, together with anomalous dispersion corrections, were taken from *International Tables for X-ray Crystallography* (Wilson 1992). In the final refinement cycle, all atoms were refined anisotropically, leading to the R_1 [$F_o > 2s(F_o)$] value 0.0432. Final atomic coordinates, equivalent isotropic displacement parameters and bond valence sums, as well as anisotropic displacement parameters, are given in Tables 4 and 5, respectively. Selected bond distances and angles are listed in Table 6.

The structure of mengxianminite is based on a closed-packed oxygen framework, with two different modules stacked along the a axis (Figs. 4 and 5). The first module (module A) consists of two O layers and one T1 layer. The O layer was made up of the edge-sharing octahedra, occupied by the cations of Al1, Al2, Al3 and Al4 (<Al-O> = 1.907-1.925 Å), each O layer contains six AlO_6 octahedra per layer in the unit-cell. The T1 layer with Al3 in octahedra and Mg/Fe in tetrahedra occurs between two O layers; it consists of two AlO_6 octahedra (<Al-O> = 1.907 Å) and four $(Mg,Fe)O_4$ tetrahedra (<Mg-O> = 1.943 Å) per layer in the unit-cell, site population refinement shows that the tetrahedral site is occupied by 0.56

Mg, 0.36 Fe and 0.08 Zn (Table 4). The second module (module B) is more complex, consists of two T2 layers and one O' layer. The T2 layer is composed of two SnO_6 octahedra (<Sn-O> = 2.077 Å), two BeO_4 tetrahedra (<BeO> = 1.668 Å), and two CaO_{11} polyhedra (<Ca-O> = 2.71 Å), the Sn octahedral site was occupied by 0.92 Sn + 0.08 Mn, and 0.81 Ca + 0.19 Na in the CaO_{11} polyhedral site (Table 4); the O' layer was made up of four AlO_6 octahedra (<Al-O> = 1.975 Å) and four BO_3 groups (<B-O> = 1.364 Å), Al5 occurs in the octahedral site, which was occupied by 0.69 Al + 0.31 Mg. As shown in Figure 5, the SnO_6 octahedra are isolated in the T2 layers; their connectivity is realized *via* BeO_4 and CaO_{11} groups. In the O' layer, AlO_6 edge-sharing octahedra form chains running along the {011} or $\{0\bar{1}1\}$ direction; these chains are connected in the c direction by the BO_3 triangular groups (Fig. 5). The cation-layer sequence in mengxianminite can be described as 4 × (O-T1-O-T2-O'-T2), the framework of mengxianminite is accordingly composed of four A modules and four B modules.

ORIGIN

Mengxianminite, ideally $Ca_2Sn_2Mg_3Al_8[(BO_3)(BeO_4)O_6]_2$, is a new Sn-bearing borate with additional O anions and without water (Strunz 06. AB. 90., Dana 24.2.8.1), showing a novel structural type belonging to the *Fdd*2 space group. To consider the origin of mengxianminite, we must first define the context offered by the Xianghualing skarn. This skarn is characterized by the presences of large amounts of Sn minerals (cassiterite, hulsite, ferronigerite-2*N*1*S*), Be minerals (hsianghualite, liberite, chrysoberyl, hambergite, bertrandite, ferrotaaffeite-2*N*'2*S*), and B minerals (fluoborite, hambergite, dravite, hulsite), reflecting

multiple Sn and Be mineralizations. Zhang and Wang (1986) indicated that the assemblages of chondrodite-phlogopite-fluoborite-hulsite were formed by the replacement of forsterite, spinel and and iron-poor augite ("fassaite"), together with cassiterite-magnetite mineralization during introduction of F- and B-rich solutions in the Xianghualing deposit, and that the Be mineralization of the Xianghualing skarn was attributed to the metasomatism and reformation processes of magnesium skarn by F- and B-rich fluids in the exocontact skarn zone.

Mengxianminite occurs as subhedral to euhedral crystals in the hsianghualite vein of the Xianghualing skarn (Fig. 1). The intimate intergrowths of mengxianminite with hsianghualite, phlogopite and fluorite indicate that it crystallized under F-rich conditions during the late stages of mineralization in the Xianghialing skarn. To our knowledge, mengxianminite (or similar synthetic compounds) has not been synthesized. On the basis of fluid inclusions studies, Liu and Zeng (1998) suggested that hsianghualite formed from 270 to 290□ and at 30−60 MPa in the Xianghualing skarn. Since mengxianminite occurs intergrown with hianghualite, these values must also represent the physical condition of mengxianminite formation. The presence of Sn and Be in the hydrothermal fluids responsible for the formation of mengxianminite is probably derived from the genetically related Laiziling granite, while B came from the wall-rocks (Tiaomajian Formation) with 284 ppm B (Zhong 2014).

IMPLICATIONS

Chemically, mengxianminite is close to minerals of nigerite group, but has lower concentrations of Al_2O_3. According to its chemical and structural features, it is also easy to distinguish mengxianminite from other Sn- and Be-bearing minerals (sørensenite and

sverigeite) and Sn- and B-bearing phases (nordenskiöldine, tusionite, vistepite) found in greisens and skarns, as well as in pegmatites and peralkaline rocks. Indeed, mengxianminite is the first borate mineral which contains both Sn and Be.

The crystal structure of mengxianminite shown in the Figure 4, is a new modular structure type with two different modules stacked along the *a* axis. The A module of mengxianminite consists of two O layers and one T1 layer, where one O layer and one T1 layer can be stoichiometrically identical to the spinel module of nigerite group minerals (Arakcheeva et al. 1995; Grey and Gatehouse1979), as well as taaffeite group minerals (Armbruster 2002). The A module of mengxianminite might be thus considered as the spinel module with an additional O layer. The intergrowths of mengxianminite with magnesiotaaffeite-2*N*'2*S* found in the Xianghualing skarn suggests these minerals sharing the same structural unit may crystallize under similar Be-, Al- and Mg- rich condition. The B module of mengxianminite is a new module, composed of two T2 layers and one O' layer (Fig. 5), showing the simplified formula $CaSnAl(BeO_4)(BO_3)$. The Ca atoms are located in a 11-coordinated polyhedron occurring between T2 layer and O' layer; the bond valence sum for Ca is 1.62 (Table 4), slightly lower than 2, indicating some light element such as Na in the 11-coordinated polyhedron site. The similar bond distance of Mg and Al in the octahedra, suggests the disordered distributions of Mg and Al in the octahedra of O' layer. However, CaO_{11} polyhedron and BO_3 groups were never reported in the modules of minerals of nigerite group, as well as taaffeite group minerals. The B module of $CaSnAl(BeO_4)(BO_3)$ in crystal structure of mengxianminite is thus a new module found in the nature.

It should be noted that the modular structure of mengxianminite can be compared to the polysomatic structures of högbomite-24*R* (Hejny and Armbruster 2002), and the *c* unit-cell parameter of mengxianminite is 5.740 Å, very similar to the *a* unit-cell parameter of phases belonging to the nigerite, högbomite and taaffeite groups (Armbruster 2002; Hejny and Armbruster 2002). Like nigerite group minerals, mengxianminite may be also one of polysomatic minerals. The chemical feature (Table 1) and structural data show that Mg can be replaced by Fe at the Mg sites, and minor Ti can enter the Sn sites. Therefore, it may be imagined that the discovery of mengxianminite draws attention to a certain expectation that Fe and Ti analogues of mengxianminite will be found in the future. In addition, similar polysomatic minerals, made up of different ratios of mengxianminite modules, could also exist.

ACKNOWLEDGEMENTS

The authors thank E.S. Grew, Daniel Atencio, Fernando Colombo and an anonymous reviewer for constructive criticism and suggestions that significantly improved the manuscript. Financial support for the research was provided by NSF of China (Grant No. 41472036), China Scholarship council (SCS), and the Fundamental Research Funds for the Central Universities.

REFERENCES CITED

Arakcheeva, A.V., Pushcharovskii, D.Y., Rastsvetaeva, R.K., Kashaev, A.A., and Nadezhina, T.N. (1995) Crystal structure of nigerite-6H. Crystallography Reports, 40, 587–592.

Armbruster, T. (2002) Revised nomenclature of högbomite, nigerite, and taaffeite minerals. European Journal of Mineralogy, 14, 389–395.

Chao, C.L. (1964) Liberite Li_2BeSiO_4, a new lithium-beryllium silicate mineral from the Nanling Ranges, South China. Acta Mineralogica Sinica 44(3), 334–342 (in Chinese with English abstract). - American Mineralogist (1965), 50, 519 (abstract).

Grey, I.E., and Gatehouse, B.M. (1979) The crystal structure of nigerite-24*R*. American Mineralogist, 64, 1255–1264.

Hejny, C., and Armbruster, T. (2002) Polysomatism in högbomite: The crystal structures of 10*T*, 12*H*, 14*T*, and 24*R* polysomes. American Mineralogist, 87, 277–292.

Huang, Y. H., Du, S.H., Wang, K.H., Zhao, C.L., and Yu, Z.Z. (1958) Hsianghualite, a new beryllium mineral. Huanan Dizhi Yu Kuangchan, 7, 35 (in Chinese). American Mineralogist (1960), 44, 1327–1328 (abstract).

Huang, Y.H., Du, S. H., and Zhou, X.Z. (1988) Hsianghualing rocks, deposits and minerals. Beijing Scientific Technique Press. 115–116 (in Chinese).

Huang, Y.H., Zhou, X.Z., Li, G.J., and Du, S.H. (1986) Mengxianminite, a new ferro-magnesium-calcium-tin-aluminum oxide mineral. Papers and Proceedings of the General Meeting - International Mineralogical Association (1986): p120 (abstract).

Krauz, W., and Nolze, G. (1996) POWDER CELL - a program for the representation and manipulation of crystal structures and calculation of the resulting X-ray powder patterns. Journal of Applied Crystallography, 29, 301–303.

Liu, J.Q., and Zeng Y.S. (1998) Preliminary study on fluid inclusions in hsianghualite. Huanan Dizhi Yu Kuangchan, 1998, 56–63.

Mandarino, J.A. (1981) The Gladstone-Dale relationship. IV. The compatibility concept and its application. Canadian Mineralogist, 19, 441–450.

Momma, K., and Izumi, F. (2011) VESTA 3 for three dimensional visualization of crystal, volumetric and morphology data. Journal of Applied Crystallography, 44, 1272–1276.

Oxford Diffraction (2007) CrysAlis CCD and CrysAlis RED, version 1.71. Oxford Diffraction, Oxford, England.

Rao, C., Hatert, F., Dal, B.F. Wang, R.C., Gu, X.P., and Baijot M. (2016) Mengxianminite, IMA 2015-070. CNMNC Newsletter No. 29, February 2016 page 200; Mineralogical Magazine, 80(1), 199–205.

Smith, D.G.W., and Nickel, E.H. (2007) A system of codification for unnamed minerals: Report of the SubCommittee for Unnamed Minerals of the IMA Commission on New Minerals, Nomenclature and Classification. Canadian Mineralogist, 45, 983–1055).

Wilson, A.J.C. (1992) International Tables for X-ray Crystallography, Vol. C. Kluwer Academic Press, London.

Yang, Z.M., Ding, K.S., Fourestier, J.D., Mao, Q., and Li, H. (2012) Ferrotaaffeite-2*N*'2*S*, a new mineral species, and crystal structure of Fe^{2+}-rich magnesiotaaffeite-2*N*'2*S* from the Xianghualing tin-polymetallic ore field, Hunan Province, China. Canadian Mineralogist, 50, 21–29.

Zhang, D.Q., and Wang, L.H. (1986) Metasomatism and zonation of the Xianghualing Tin-polymetallic deposit. Bulletin of the Institute of Mineral Deposits Chinese Academy of Geological Sciences, 2, 144–154.

Zhong, J.L. (2014) Major types and prospecting direction of nonferrous and rare polymetallic ore deposit in Xianghualing area, South China. Geology and mineral resource of south China, 30(2), 99–108.

Zhu, J.C., Wang, R.C., Lu,J.J., Zhang, H., Zhang, W.L., Xie, L., and Zhang, R.Q. (2011) Fractionation, Evolution, Petrogenesis and Mineralization of Laiziling Granite Pluton, Southern Hunan Province. Geological Journal of China Universities,17(3), 381–392.

Figure captions:

FIGURE 1. BSE image (a) and photomicrograph (b) showing the occurrence and mineral associations of mengxianminite in the Xianghualing skarn. Abbr.: Mxm - mengxianminite, Fl - fluorite, Phl - phlogopite, Hsh - hsianghualite, Mag - magnetite, Cas - cassiterite.

FIGURE 2. The Raman spectrum of mengxianminite.

FIGURE 3. The infrared spectrum of mengxianminite.

FIGURE 4. The crystal structure of mengxianminite, drawn using the VESTA 3 program (Momma and Izumi, 2011).

FIGURE 5. An enlarged view of a portion of the mengxianminite structure, showing the connectivity in the A module (O-T1-O) and B module (T2-O'-T2). Drawn using the VESTA 3 program (Momma and Izumi 2011). For key, see Figure 4.

Table captions:

TABLE 1. Chemical composition of mengxianminite for the Xianghualing skarn

TABLE 2. X-ray powder diffraction pattern of mengxianminite (d in Å)

TABLE 3. Crystallographic data and refinement parameters for mengxianminite

TABLE 4. Final atomic coordinates, equivalent isotropic displacement parameters and bond valence sums (BVS) for mengxianminite

TABLE 5. Anisotropic displacement parameters for mengxianminite (in $Å^2$)

TABLE 6. Selected bond distances (Å) in mengxianminite

412
413
414

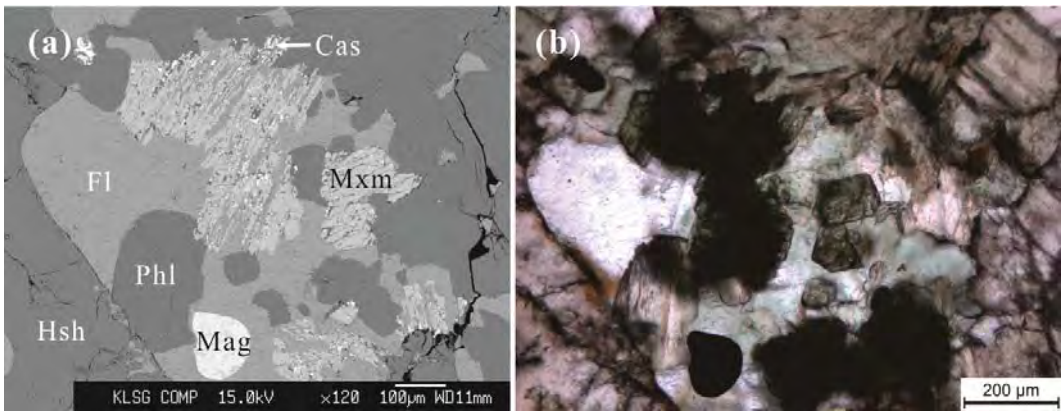

FIGURE 1. BSE image (a) and photomicrograph (b) showing the occurrence and mineral associations of mengxianminite in the Xianghualing skarn. Abbr.: Mxm - mengxianminite, Fl - fluorite, Phl - phlogopite, Hsh - hsianghualite, Mag - magnetite, Cas - cassiterite.

415
416
417
418
419
420
421
422

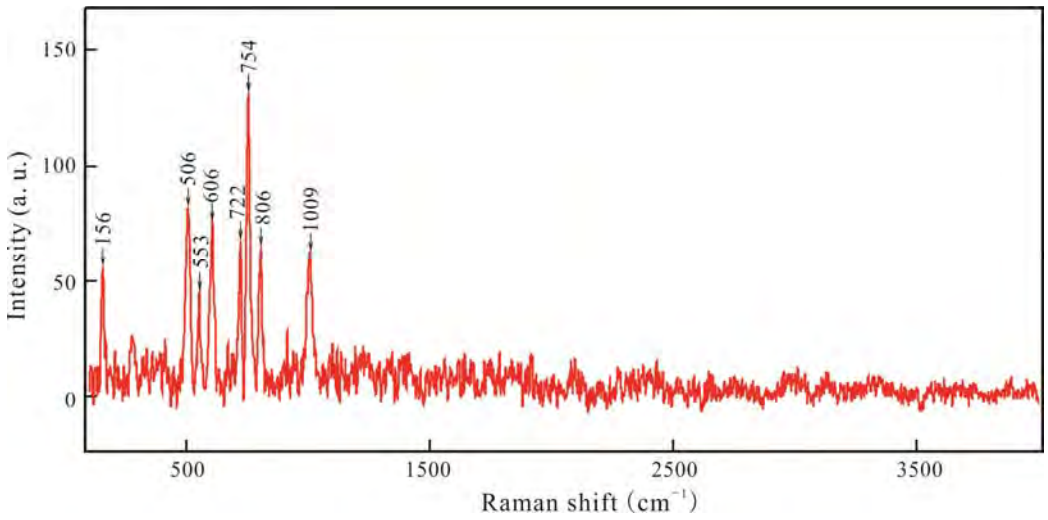

FIGURE 2. The Raman spectrum of mengxianminite.

423
424
425
426

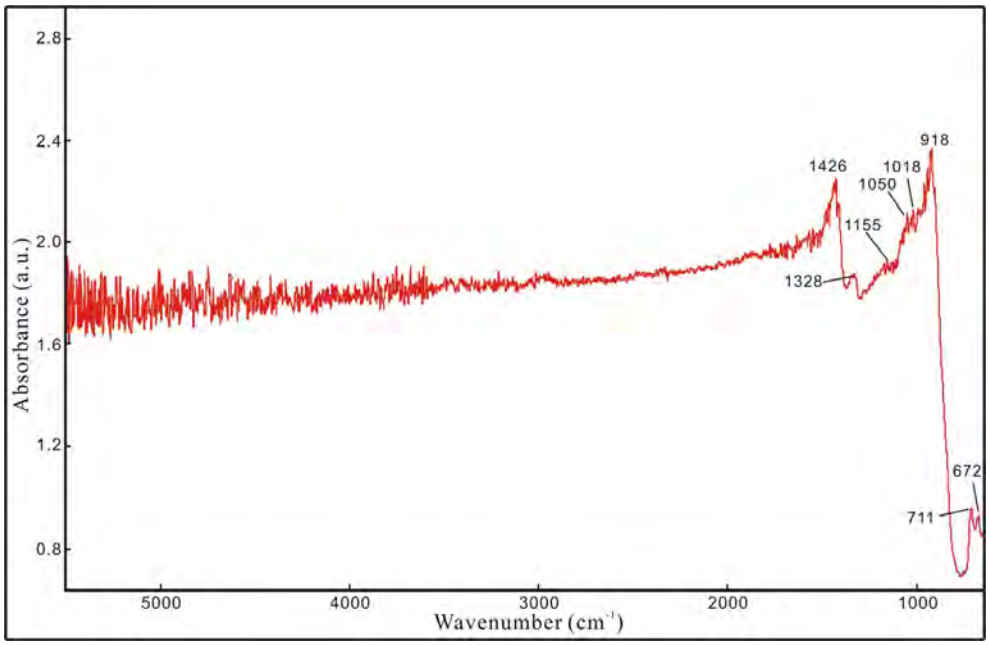

FIGURE 3. The infrared spectrum of mengxianminite.

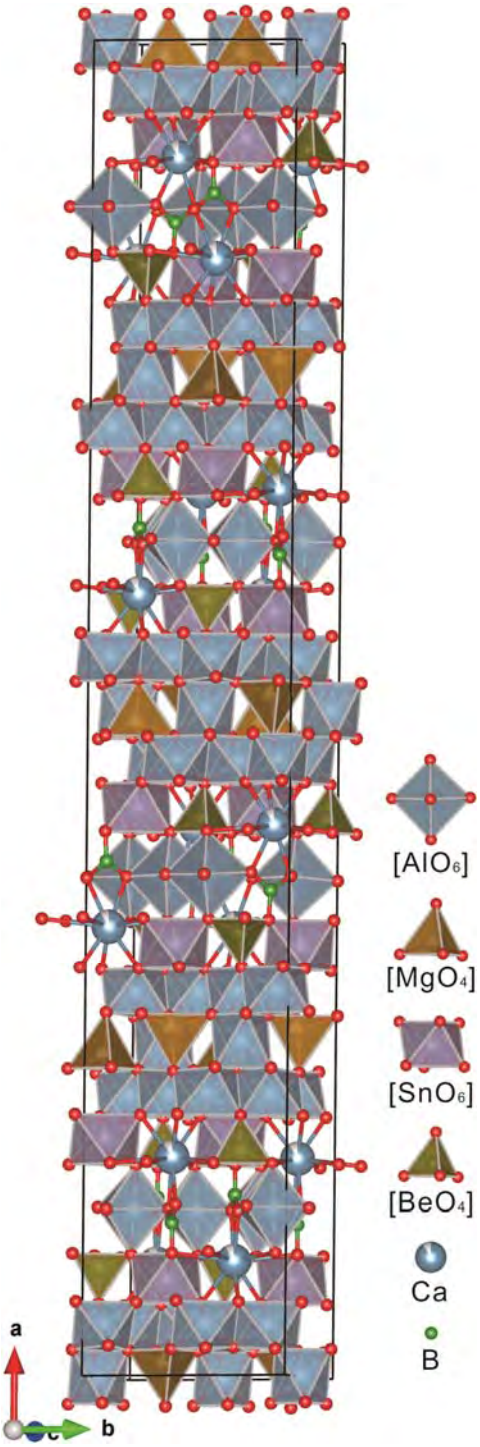

FIGURE 4. The crystal structure of mengxianminite, drawn using the VESTA 3 program (Momma and Izumi, 2011).

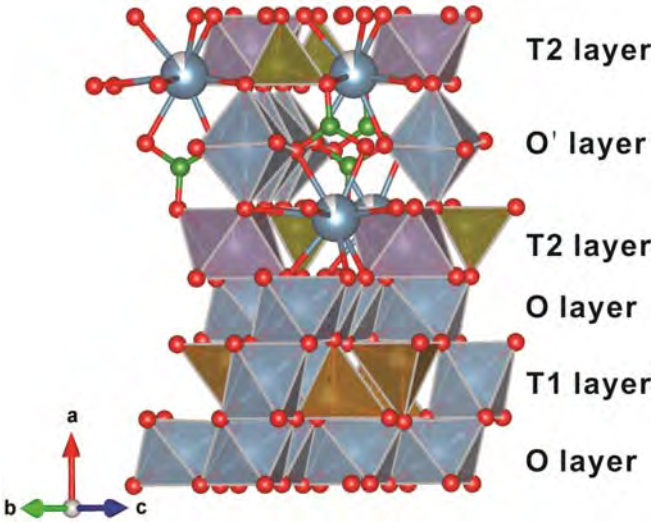

FIGURE 5. An enlarged view of a portion of the mengxianminite structure, showing the connectivity in the module A (O-T1-O) and module B (T2-O'-T2). Drawn using the VESTA 3 program (Momma and Izumi 2011). For key, see Figure 4.

TABLE 1. Chemical composition of mengxianminite for the Xianghualing skarn

	Wt%	Range	Std. dev.		*a.p.f.u.*
Al_2O_3	40.00	39.66-40.64	0.39	Al	8.423
SnO_2	25.96	25.46-26.54	0.44	Sn	1.850
CaO	8.56	8.11-9.18	0.43	Ca	1.637
MgO	6.57	5.86-7.75	0.74	Mg	1.748
FeO	4.83	4.58-5.24	0.23	Fe	0.721
B_2O_3*	6.53	-		B	2.014
BeO*	4.37	-		Be	1.876
ZnO	1.81	1.21-2.24	0.38	Zn	0.238
MnO	1.23	1.09-1.42	0.13	Mn	0.186
Na_2O	1.13	0.77-1.40	0.28	Na	0.393
SiO_2	0.04	0.02-0.05	0.01	Si	0.007
K_2O	0.00	0-0.01	0.00	K	0.000
TiO_2	0.10	0.01-0.22	0.08	Ti	0.014
Total	101.12				

* The B_2O_3 and BeO contents were measured by secondary ion mass spectrometry. Structural formulas were calculated on the basis of O = 26 atoms.

510 **TABLE 2.** X-ray powder diffraction pattern of mengxianminite (d in Å)

$I_{obs.}$	$d_{obs.}$	$I_{calc.}$	$d_{calc.}$	*hkl*
-	-	74	7.604	8 0 0
-	-	39	4.307	7 1 1
20	4.04	41	3.998	9 1 1
17	3.63	38	3.692	11 1 1
35	3.00	43	3.008	16 2 0
100	2.931	78	2.902	17 1 1
25	2.842	46	2.858	2 0 2
		100	2.844	1 3 1
9	2.781	14	2.772	5 3 1
		22	2.762	6 0 2
28	2.714	16	2.706	7 3 1
		78	2.690	19 1 1
-	-	35	2.587	20 2 0
20	2.515	12	2.535	24 0 0
		32	2.531	11 3 1
29	2.475	34	2.479	0 2 2
30*	2.430	87	2.432	13 3 1
-	-	60	2.408	6 2 2
100	2.375	85	2.395	14 0 2
		41	2.390	6 4 0
-	-	55	2.330	15 3 1
20	2.281	11	2.280	10 4 0
-	-	23	2.154	14 2 2
15	2.071	21	2.077	16 2 2
		10	2.065	16 4 0
52	2.028	13	2.031	21 3 1
**	1.933	32	1.922	20 2 2
15	1.859	15	1.854	4 4 2
35	1.807	2	1.810	9 1 3
17	1.727	8	1.729	13 5 1
		13	1.728	33 1 1
16	1.603	15	1.592	20 4 2
18	1.566	71	1.570	30 2 2
		42	1.564	30 4 0
98*	1.530	18	1.534	14 6 0
		10	1.531	15 3 3

511 * overlapping with phlogopite. ** overlapping with fluorite.

512

513

514

515

TABLE 3. Crystallographic data and refinement parameters for mengxianminite

Crystal size (mm)	0.139 x 0.108 x 0.088
Color	green
Space group	*Fdd2*
a, *b*, *c* (Å)	60.699 (4), 9.914 (1), 5.745 (1)
V (Å^3)	3457.4 (4)
Z	8
D(calc) (g/cm³)	4.170(calc.)
$2\theta_{min}$, $2\theta_{max}$	5.36°, 57.48°
Range of indices	$-82 \le h \le 77$, $-13 \le k \le 12$, $-7 \le l \le 7$
Measured intensities	7315
Unique reflections	2063
Independent non-zero [$I > 2\sigma(I)$] reflections	1722
Refined parameters	193
R_1 [$F_0 > 2\sigma(F_0)$]	0.0432
R_1 (all)	0.0594
wR_2 (all)	0.0844
S (goodness of fit)	1.055
Max Δ/σ in the last l.s. cycle	0.001
Max peak and hole in the final ΔF map (*e*/Å^3)	+1.08 and –0.85

TABLE 4. Final atomic coordinates, equivalent isotropic displacement parameters and bond valence sums (BVS) for mengxianminite

Atom	Layer	*X*	*Y*	*Z*	U_{eq}	BVS
Sn	T2	0.572538(9)	0.82975(6)	-0.6547(2)	0.00931(15)	3.72
Mg	T1	0.51025(3)	0.8333(2)	0.3371(6)	0.0096(5)	2.12
Ca	T2	0.58662(3)	0.6614(2)	-0.1507(10)	0.0175(6)	1.74
Al1	O	0.53869(4)	0.5824(3)	0.5907(13)	0.0101(5)	2.90
Al2	O	0.53871(3)	0.8324(3)	-0.1616(9)	0.0099(5)	2.90
Al3	T1	0.5	0.5	0.3361(9)	0.0111(7)	3.01
Al4	O	0.53854(3)	0.5838(3)	0.0883(12)	0.0094(5)	2.86
Al5	O’	0.62505(4)	0.4188(3)	0.0792(11)	0.0126(9)	2.59
Be	T2	0.66786(16)	0.7580(12)	-0.441(2)	0.008(2)	1.86
B	O’	0.63570(14)	0.6693(11)	-0.173(3)	0.012(2)	3.04
O1		0.52004(8)	0.9249(7)	0.612(3)	0.015(2)	1.95
O2		0.52010(9)	0.9259(7)	0.0557(14)	0.013(2)	1.98
O3		0.55514(8)	0.5075(6)	-0.1692(19)	0.0108(14)	1.926
O4		0.51997(8)	0.6469(6)	0.339(3)	0.0138(14)	2.48
O5		0.55522(9)	0.7431(6)	-0.396(2)	0.0130(13)	1.99
O6		0.65819(9)	0.6739(8)	-0.185(3)	0.019(2)	1.933
O7		0.55505(9)	0.7467(6)	0.0720(16)	0.0118(14)	2.20
O8		0.62469(11)	0.6116(7)	0.0028(11)	0.0193(16)	1.86
O9		0.55529(8)	0.5004(7)	0.3305(18)	0.0105(13)	1.74
O10		0.65806(9)	0.4121(7)	0.065(2)	0.015(2)	2.05
O11		0.62279(10)	0.7261(7)	-0.3461(12)	0.0185(18)	1.74
O12		0.52210(8)	0.6663(7)	-0.159(3)	0.0155(12)	1.91
O13		0.59206(8)	0.4282(7)	0.089(3)	0.0174(13)	1.72

Occupancy: Sn = 0.92 Sn + 0.08 Mn; Mg = 0.56 Mg + 0.36 Fe + 0.08 Zn;
Ca = 0.81 Ca + 0.19 Na; Al5 = 0.69 Al + 0.31 Mg.

560
561
562
563
564

TABLE 5. Anisotropic displacement parameters for mengxianminite (in $Å^2$)

Atom	U_{11}	U_{22}	U_{33}	U_{23}	U_{13}	U_{12}
Sn	0.0100(2)	0.0080(2)	0.0094(3)	0.0004(3)	-0.0002(4)	0.0002(3)
Mg	0.0109(8)	0.0077(8)	0.010(1)	-0.0007(9)	0.001(1)	-0.001(1)
Ca	0.0123(9)	0.017(1)	0.023(1)	-0.002(1)	-0.001(2)	-0.0001(9)
Al1	0.011(1)	0.009(1)	0.010(1)	-0.0052)	0.003(3)	-0.000(1)
Al2	0.011(1)	0.008(1)	0.011(1)	-0.001(1)	0.000(2)	-0.001(1)
Al3	0.012(1)	0.012(2)	0.010(2)	0	0	0.001(2)
Al4	0.009(1)	0.008(1)	0.011(1)	-0.006(2)	-0.000(2)	-0.000(1)
Al5	0.012(1)	0.013(1)	0.013(2)	0.003(1)	-0.002(2)	-0.001(1)

565
566
567

TABLE 6. Selected bond distances (Å) in mengxianminite

Sn-O3	2.056(6)	Al1-O3	1.858(11)	Al2-O5	1.897(10)
Sn-O5	2.014(9)	Al1-O5	1.884(7)	Al2-O7	1.873(9)
Sn-O7	2.066(8)	Al1-O9	1.978(10)	Al2-O9	1.947(7)
Sn-O13	2.079(12)	Al1-O12	1.940(15)	Al2-O12	1.931(7)
Sn-O6	2.200(11)	Al1-O2	1.929(7)	Al2-O2	1.922(8)
Sn-O10	2.045(6)	Al1-O4	1.946(1)	Al2-O1	1.954(11)
<Sn-O>	2.077	<Al-O>	1.923	<Al-O>	1.921
Al4-O3	1.943(11)	Al5-O13	2.006(6)	Ca-O3	2.448(6)
Al4-O7	1.903(7)	Al5-O8	1.961(8)	Ca-O5	2.504(9)
Al4-O9	1.911(10)	Al5-O8’	1.959(10)	Ca-O7	2.455(8)
Al4-O12	1.921(15)	Al5-O11	1.955(10)	Ca-O13	2.713(13)
Al4-O4	1.934(14)	Al5-O11’	1.963(8)	Ca-O13’	3.055(12)
Al4-O1	1.940(7)	Al5-O10	2.007(6)	Ca-O6	2.899(11)
<Al-O>	1.925	<Al-O>	1.975	Ca-O6’	2.884(12)
Mg-O12	1.964(5)	Be-O6	1.787(17)	Ca-O8	2.522(7)
Mg-O2	1.953(8)	Be-O9	1.637(11)	Ca-O11	2.548(7)
Mg-O4	1.940(6)	Be-O13	1.607(19)	Ca-O10	2.694(1)
Mg-O1	1.916(13)	Be-O10	1.640(13)	Ca-O10	3.088(10)
<Mg-O>	1.943	<Be-O>	1.668	<Ca-O>	2.71
B-O6	1.368(9)	Al3-O2×2	1.903(8)		
B-O8	1.338(15)	Al3-O4 ×2	1.895(6)		
B-O11	1.387(14)	Al3-O1 ×2	1.922(11)		
<B-O>	1.364	<Al-O>	1.907		

568